Full field vertical scanning in short coherence digital holographic microscope

Zahra Monemhaghdoust,[1,*] Frederic Montfort,[1,2] Etienne Cuche,[2] Yves Emery,[2] Christian Depeursinge,[3] and Christophe Moser[1]

[1]*Ecole Polytechnique Fédérale de Lausanne, Laboratory of Applied Photonics Devices, CH-1015 Lausanne, Switzerland*

[2]*Lyncée Tec SA, CH-1015 Lausanne, Switzerland*

[3]*Ecole Polytechnique Fédérale de Lausanne, Laboratoire d'Optique Appliquée, CH-1015 Lausanne, Switzerland*

**zahra.monemhaghdoust@epfl.ch*

Abstract: In Digital holography Microscopes (DHM) implemented in the so-called "off axis" configuration, the object and reference wave fronts are not co-planar but form an angle of a few degrees. This results into two main drawbacks. First, the contrast of the interference is not uniform spatially when the light source has low coherence. The interference contrast is optimal along a line, but decreases when moving away from it, resulting in a lower image quality. Second, the non-coplanarity between the coherence plane of both wavefronts impacts the coherence vertical scanning measurement mode: when the optical path difference between the signal and the reference beam is changed, the region of maximum interference contrast shifts laterally in the plane of the objective. This results in more complex calculations to extract the topography of the sample and requires scanning over a much larger vertical range, leading to a longer measurement time. We have previously shown that by placing a volume diffractive optical element (VDOE) in the reference arm, the wavefront can be made coplanar with the object wavefront and the image plane of the microscope objective, resulting in a uniform and optimal interferogram. In this paper, we demonstrate a vertical scanning speed improvement by an order of magnitude. Noise in the phase and intensity images caused by scattering and non-uniform diffraction in the VDOE is analyzed quantitatively. Five VDOEs were fabricated with an identical procedure. We observe that VDOEs introduce a small intensity non-uniformity in the reference beam which results in a 20% noise increase in the extracted phase image as compared to the noise in extracted phase image when the VDOE is removed. However, the VDOE has no impact on the temporal noise measured from extracted phase images.

OCIS codes: (050.1950) Diffraction gratings; (090.1995) Digital holography; (110.0180) Microscopy; (110.4280) Noise in imaging systems.

References and links

1. E. Cuche, P. Marquet, and C. Depeursinge, "Simultaneous amplitude-contrast and quantitative phase-contrast microscopy by numerical reconstruction of Fresnel off-axis holograms," Appl. Opt. **38**(34), 6994–7001 (1999).
2. E. Cuche, F. Bevilacqua, and C. Depeursinge, "Digital holography for quantitative phase-contrast imaging," Opt. Lett. **24**(5), 291–293 (1999).
3. U. Schnars and W. Jüptner, "Digital recording and numerical reconstruction of holograms," Meas. Sci. Technol. **13**(9), 85–101 (2002).
4. F. Dubois, L. Joannes, and J. C. Legros, "Improved three-dimensional imaging with a digital holography microscope with a source of partial spatial coherence," Appl. Opt. **38**(34), 7085–7094 (1999).
5. H. Ding and G. Popescu, "Diffraction phase contrast microscopy," Opt. Express **18**(2), 1569–1575 (2010).
6. P. Kolman and R. Chmelik, "Coherence-controlled holographic microscope," Opt. Express **18**, 21990 (2010).

#188965 - $15.00 USD Received 17 Apr 2013; accepted 2 May 2013; published 15 May 2013

7. F. Dubois and C. Yourassowsky, "Full off-axis red-green-blue digital holographic microscope with LED illumination," Opt. Lett. **37**(12), 2190–2192 (2012).
8. S. Kosmeier, P. Langehanenberg, G. Bally, and B. Kemper, "Reduction of parasitic interferences in digital holographic microscopy by numerically decreased coherence length," Appl. Phys. B **106**(1), 107–115 (2012).
9. A. Harasaki, J. Schmit, and J. C. Wyant, "Improved vertical-scanning interferometry," Appl. Opt. **39**(13), 2107–2115 (2000).
10. Z. Monemhaghdoust, F. Montfort, Y. Emery, C. Depeursinge, and C. Moser, "Dual wavelength full field imaging in low coherence digital holographic microscopy," Opt. Express **19**(24), 24005–24022 (2011).

1. Introduction

Digital holographic microscopy is a quantitate phase contrast technology with numerous applications thanks to its ability to digitally reconstruct objects at different depths [1–3]. Additionally, thanks to the ability of reconstructing complex wave fields, digital holography offers the opportunity to numerically subtract or superimpose fields or phase distributions that correspond to different wavelengths. The subtraction of phase distributions from reconstructed wave fields of specimens that have been recorded at two different wavelengths results in a synthetic longer wavelength. Thus, with multiple illumination wavelengths, the measurement range is extended without phase ambiguities.

Due to the long coherence length of laser light, optical path length resolution in laser based digital holographic microscopy suffers from parasitic interferences caused by multiple reflections within the experimental setup. To counter this phase noise, several configurations were proposed with optical sources of partial coherence [4–6]. In [7] an RGB DHM with LED illumination was proposed to reduce the noise thanks to the partial temporal and spatial coherences that enables off-axis configuration for fast acquisition mode. But on the other hand, use of short coherent light requires precise and stable matching of object and reference arm's optical path length (OPL) and limits the field of view in off-axis holography [8]. In the off-axis configuration, there is a non-zero angle between the object and reference beams that enables the complex amplitude computation from only one recorded hologram. The latter is an advantage for the analysis of rapidly varying samples.

In addition to reducing coherent noise, the use of short coherence (e.g. <20 μm) provides depth slicing, i.e., rejecting signals which come from a depth larger than the source coherence length. This coherence gating is used in Optical Coherence Tomography or Microscopy (OCT/OCM) to provide depth images in diffuse sample. Similarly, vertical scanning interferometry is a widely-used method based on common-path optical coherence gating to measure three-dimensional surface topography with nanometric resolution [9].

The concepts of coherence gating can also be applied to an off-axis DHM as it is shown in this paper. A short coherence length of the source yields high-contrast fringes only at the positions where the OPL difference is zero. However, due to the small angle (γ shown in Fig. 1(b)) between reference and object beams in an off-axis configuration of the DHM, interference fringes are present only in a slice of the field of view for each focus position. For a given object depth, this requires scanning the optical path length to an extent such that the slice moves across the full field of view (d_{scan} in Figs. 1(a) and 1(b)). This translates to a longer scan range than the object depth. Figures 1(a) and 1(b) show the position of coherence planes at the start and end of scanning, respectively. In Fig. 1, l_c is the coherence length of the beams. However, as it is shown in Fig. 1(c), by introducing a tilt equal to γ in the coherence plane of the reference beam, the coherence plane of the object and reference beam overlap over the full field of view in a way similar to on-axis interferometry. In this case, the scanning range required is of the order of the object depth. Thus, the scanning range required, in optical coherence measurements, for the off-axis geometry with an engineered coherence plane is expected to be similar to that required in common-path interferometers.

#188965 - $15.00 USD Received 17 Apr 2013; accepted 2 May 2013; published 15 May 2013

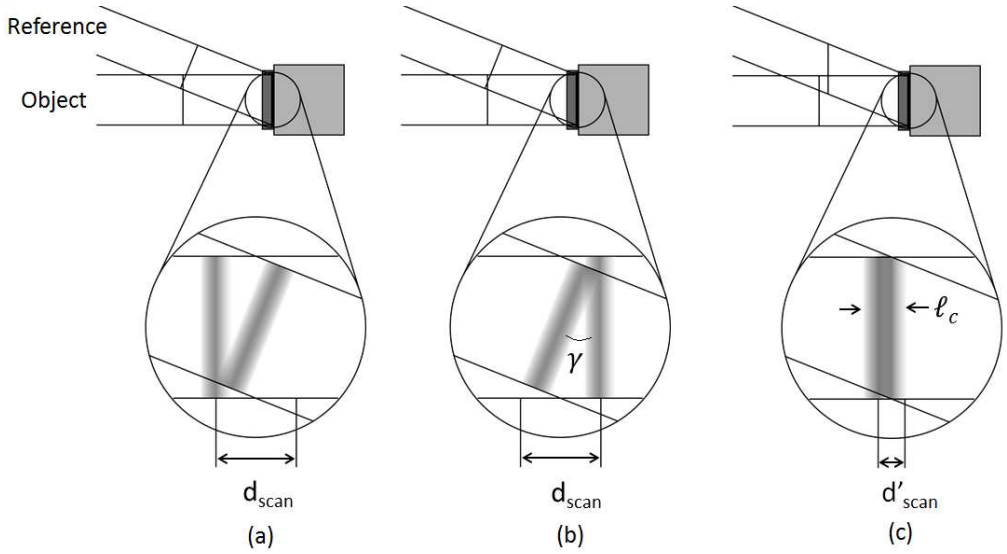

Fig. 1. Vertical scanning. (a), (b) without, and (c) with, reference beam coherence plane tilt manipulation.

We have recently introduced [10] a method based on a volume diffractive element (VDOE) to correct the coherence plane tilt in off-axis DHM. The VDOE consists of two phase gratings recorded on a photopolymer (BAYFOL® HX) from Bayer MaterialScience AG, each laminated on one side of a wedge prism. The VDOE is placed in the reference arm of an off-axis DHM to introduce a small tilt γ in the coherence plane of the reference without any effect on the propagation direction, as it is shown in Fig. 2(a). The tilt introduced in the coherence plane provides full field of view imaging in the off-axis DHM. An image of the device is shown in Fig. 2(b).

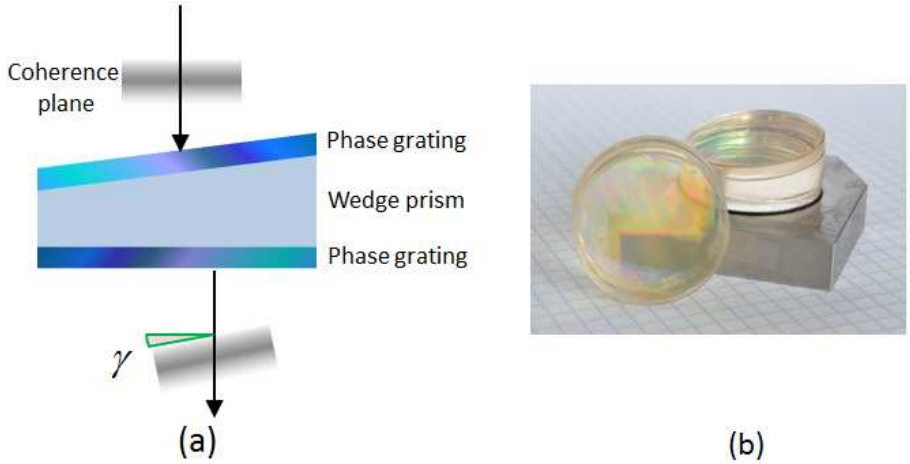

Fig. 2. (a) VDOE which preserves the propagation direction and introduces a slight angle in coherence plane. (b) Fabricated device.

In the construction of the VDOE, care is taken to match the refractive index at interfaces to avoid parasitic Fresnel reflections. The VDOE introduces its own parasitic noise in the system due to scattering by the holographic medium and inhomogeneities in the diffracted field. In this paper, we analyze quantitatively the spatial and temporal noise introduced in the intensity and phase image by the VDOE. Five VDOEs were fabricated according to an

#188965 - $15.00 USD Received 17 Apr 2013; accepted 2 May 2013; published 15 May 2013

identical procedure and inserted into a commercial DHM. For spatial noise in the image (intensity or phase), the parameters of interest are the mean roughness (R_a) and the maximum roughness (R_t). R_a is defined as the average of the absolute values of the difference between the measurement and the mean and R_t as the highest peak to valley value. Temporal standard deviations are measured to analyze the temporal phase noise in the extracted phase images.

Section 2 presents the results of the spatial and temporal phase noise caused by the VDOEs. In section 3, we demonstrate the improvement gained in vertical coherence scanning mode in a DHM retrofitted with a VDOE.

2. Quantification of the spatial and temporal phase noise

2.1. Experimental set up

The optical set-up of the DHM is shown in Fig. 3. Two low coherence sources of different wavelengths (λ_1 = 685 nm, $\Delta\lambda_1$ = 9.1 nm, λ_2 = 794 nm, $\Delta\lambda_2$ = 15.2 nm) are combined and split into two beams by a first beam splitter. One beam is split again in its two spectral components (reference beam 1 and 2). The other one illuminates the object through a microscope objective. The reflected light from the sample is recombined with the two reference beams on the camera. Two delay lines equalize the optical path difference between the two references and the object paths. The object and reference beams interfere in off-axis geometry. The object beam is normal to the camera, whereas an angle w.r.t normal is introduced for the reference beams. The plane defined by the direction of the object beam and reference 1 is orthogonal to the one defined by the object beam and reference 2. The hologram records the interference at both wavelengths simultaneously. This geometry enables Fourier filtering of the frequencies for each wavelength, in one hologram and thus maintains fast measurements.

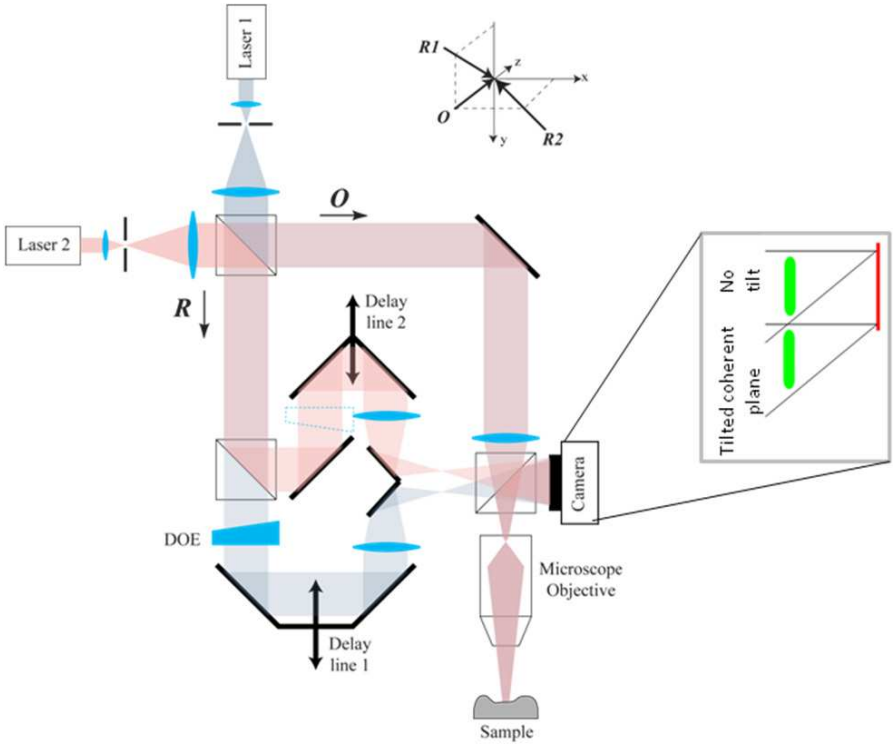

Fig. 3. Optical set-up of the digital holographic microscope.

#188965 - $15.00 USD Received 17 Apr 2013; accepted 2 May 2013; published 15 May 2013

2.2. Intensity and phase noise analysis

To evaluate the performance of the VDOE and the reproducibility of the recording process, five VDOEs were recorded with identical parameters for use at a single wavelength 794nm and inserted into the reference arm of the DHM. The reference beam uniformity was characterized using the standard deviation of its intensity over the complete field of view of the CCD (1024x1024 pixels). The reference intensity image is captured with a shutter time set to a value for which the highest pixel intensity is saturated. The results of this measurement on the image reference intensity after the VDOE are shown in Table 1. The values represent the relative change of the standard deviation in images obtained with and without VDOE.

Table 1. Relative change of standard deviation of the reference beam obtained without and with the VDOE in the path of reference beam.

	Std Dev
1	+ 17%
2	+ 47%
3	+ 14%
4	+ 17%
5	–0.9%

The results show that on average, the VDOE introduce a small but measurable intensity non-uniformity on the reference beam.

In the following, the spatial and temporal phase noise are analyzed on reconstructed phase images. The object used in this analysis is a planar mirror.

To quantify the spatial phase noise introduced by the VDOE, five regions of interest composed of 70x70 pixels are selected in the image (regions 1 to 5 in Fig. 4). The mean roughness (R_a) and maximum roughness (R_t) are evaluated on each of the five regions. Measurements are performed on non-calibrated reconstructed phase images (i.e no reference hologram is taken). The reconstructed wavefront contains the influence of all the optical elements in the set-up. The roughness parameters are evaluated on a surface resulting from the subtraction of a 5th order polynomial fit to the original measured surface. This procedure enables to evaluate the medium and high frequency perturbations due to the VDOE.

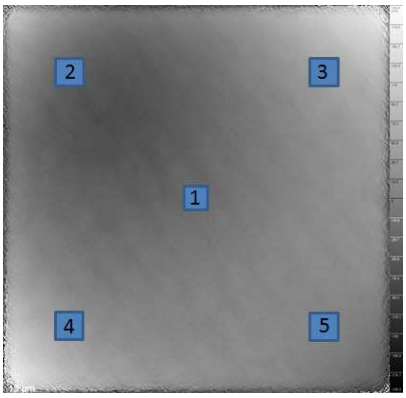

Fig. 4. Example phase image resulting from the subtraction of a 5th order polynomial fit from the original phase image. Regions 1 to 5 of size 70 x 70 pixels are used to characterize the spatial phase.

#188965 - $15.00 USD Received 17 Apr 2013; accepted 2 May 2013; published 15 May 2013

Table 2. Mean roughness (R_a) and maximum roughness (R_t) measured in five VDOES (top to bottom in the table) over five region of interest (left to right in the table) in the phase image of Fig. 4. Values represent the relative change obtained without and with the VDOE placed in the path of the reference arm.

Region	1		2		3		4		5	
VDOE	*Ra*	*Rt*	*Ra*	*Rt*	*Ra*	*Rt*	*Ra*	*Rt*	*Ra*	*Rt*
1	5%	8.8%	–27%	–20%	18%	22%	11%	–10%	34%	47%
2	1.2%	19%	–26%	–29%	15%	1.7%	2.5%	–21%	19%	28%
3	5%	14%	–34%	–32%	0.9%	–7.1%	–8.4%	–12%	27%	49%
4	7.5%	8.8%	–31%	–36%	3.8%	–6.2%	–11%	–29%	16%	28%
5	0%	7.9%	–32%	–35%	4.8%	–3.3%	–8.4%	–25%	3.6%	4%

The results in Table 2 show that by some process improvement in the manufacturing of the VDOE, a spatial phase noise comparable with the results without the VDOE can be obtained (grating # 5), likely because of the reduction of parasitic interferences.

These measurements give information on the perturbations of the wavefront induced by the VDOE. However these effects can be included in a calibrated hologram prior to making an actual measurement. To quantify this, measurements were performed on a calibrated system. The calibration is done by acquiring a reference hologram using an ultra-flat mirror and subtracting the reconstructed wavefront of this reference hologram to the one obtained on the measured sample (with and without VDOE). This procedure enables the remaining wavefront to be only due to the sample and eliminates all other wavefront distortions due to the setup, including the spatial perturbations due to the VDOE that were quantified above. One of the VDOEs was inserted into the second reference arm of the DHM (794 nm with short coherence length of 18 µm: reference 2 in Table 3). The light source in the first reference arm of the DHM is 666 nm with a long coherence length of 195 µm. There is no VDOE in this arm. Figure 5 shows the reconstructed phase image with the VDOE.

The temporal phase noise is measured in the six regions shown in Fig. 5. Each region contains 2x2 pixels and the standard deviation is measured over 50 images in 10 seconds with an acquisition rate of 5 images per second.

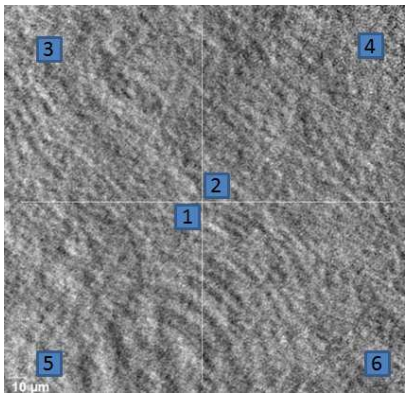

Fig. 5. Phase image resulting from subtraction of the original phase image with the reference phase hologram Selected regions 1 to 6 of size 2 x 2 pixels used to characterize the temporal phase noise.

#188965 - $15.00 USD Received 17 Apr 2013; accepted 2 May 2013; published 15 May 2013

Table 3. Temporal standard deviation measured in [nm] in five regions shown in Fig. 5.

Region	reference 1(666nm)	reference 2(794nm)
	without VDOE	with VDOE
1	0.50	0.72
2	0.61	0.62
3	0.85	0.79
4	1.08	0.93
5	0.70	0.78
6	0.77	0.78
Average	0.752	0.77
Std. Dev.	0.202	0.10

The measurements show that although the average temporal standard deviation over six regions remains unchanged with or without the VDOE (0.77 nm vs 0.75 nm), the phase values with VDOE are more uniform (0.1 vs 0.22 Std. Dev). We believe this is due to a constant fringe contrast over the image, whereas without VDOE, the fringe contrast is worse in the corners. This measurement confirms that a reference hologram with VDOE is stable and can be used in a calibrated system.

3. Full field high speed vertical scanning

In vertical scanning, high contrast fringes are obtained only when the two paths of the interferometer are closely matched in length. Thus, if in the interference microscope the path length of the sample arm of the interferometer is varied, the height variations across the sample can be determined by looking at the sample position for which the fringe contrast is maximum. In this measurement there are no height ambiguities, however, only a single surface height is being measured at a time and a large number of measurements and calculations are required to determine a large range of surface height values. As it can be understood from Fig. 1, the number of height measurements becomes larger if there is mismatch in the coherence planes between the reference and object beams. The number of height measurements is minimum when the coherence planes are parallel, as we show below.

A VDOE recorded for the wavelength 794 nm was placed in the reference arm of the DHM and a step target with step heights of 10 nm, 100 nm, 1 μm, 2 μm, and 4 μm, was used as the sample. The height measurements were compared with and without the VDOE. Since the coherence plane is tilted without the VDOE, the scanning has to be done over a longer axial range so that it covers not only the sample height, but also the height due to the inclination of the coherence plane over the whole field of view. Whereas with the VDOE, the scanning plane is parallel to the sample and the scanning range is reduced to the sample height. The measurements show that the scanning range is reduced by a factor of 10 which translates into one order of magnitude faster measurements. This result is in agreement with the calculations: the scanning range is given by, $d_{scan} = w*\tan(\gamma) = 400$ μm (w is the camera chip size which is 9.3 mm and coherence plane tilt is γ is 2.5°), and the minimum scanning distance is twice the coherence length of the source $d'_{scan} = 2*l_c = 40$ μm, which is 1/10th the scanning range without VDOE. Vertical scanning was done by continuously moving the sample by changing the stepper motor position in steps of 1 μm. In this way, several interferograms are recorded and their intensity images are reconstructed. Then, the intensity images are analyzed pixel by pixel. For each pixel, the motor position for which the maximum fringe contrast amplitude is realized, represents the height value. Figure 6

#188965 - $15.00 USD Received 17 Apr 2013; accepted 2 May 2013; published 15 May 2013

illustrates the procedure. Figure 7 shows the line profile and the image of the staircase sample.

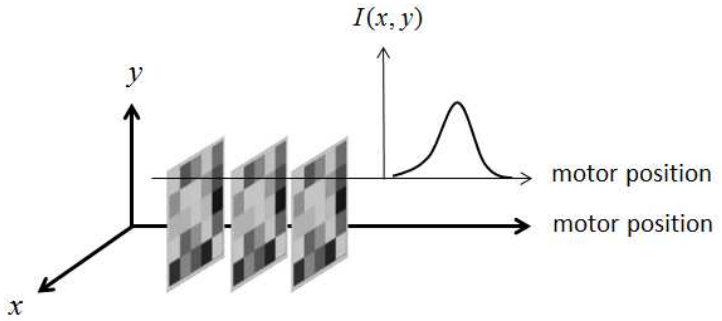

Fig. 6. Vertical scanning procedure.

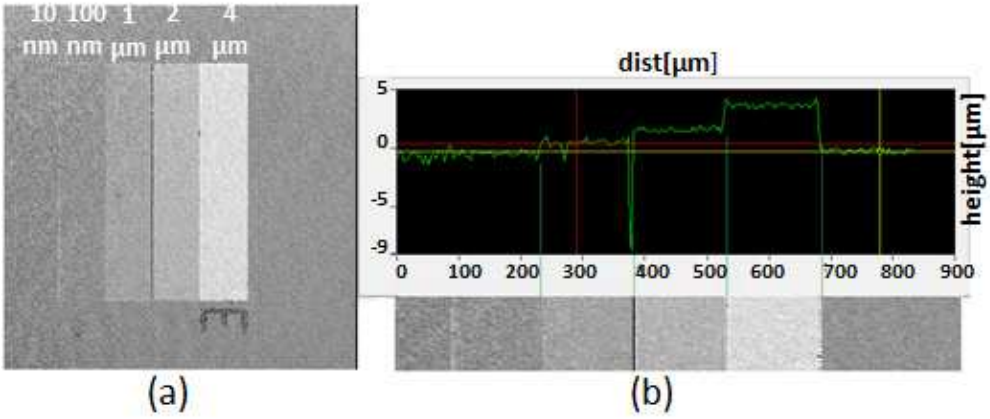

Fig. 7. (a) The resulting image obtained by the vertical scanning measurements which provides (b) the height line profile of the staircase sample.

4. Conclusion

Coherent phase noise introduced by the VDOEs in the intensity and phase measurements was studied and experimentally quantified in a DHM set-up using five VDOE fabricated with an identical procedure. Spatial noise was shown to be slightly larger with the VDOE inserted, however these perturbations are cancelled out by using a reference calibration hologram which, we have shown, is stable in time. Thus the VDOE provides a coherence plane tilt to generate full field images in a low coherence off-axis DHM without introducing significant noise in the extracted phase image. The coplanarity of the coherence plane of reference and image beams, enabled by the VDOE, permits to acquire a vertical coherence scan with the minimum amount of measurements (camera frames).

Acknowledgments

The authors would like to acknowledge the support from CTI (Commission for Technology and Innovation) 13366.1 PFFLE-NM in Switzerland.